J|A|C|S COMMUNICATIONS

Published on Web 06/07/2010

Assembly of Fullerene-Carbon Nanotubes: Temperature Indicator for Photothermal Conversion

Yanfei Shen,[†,§] Andre G. Skirtach,[†] Tomohiro Seki,[‡] Shiki Yagai,[‡] Hongguang Li,[†] Helmuth Möhwald,[†] and Takashi Nakanishi*[,†,§,⊥]

Max Planck Institute of Colloids and Interfaces, 14424 Potsdam, Germany, Chiba University, 1-33 Yayoi-cho, Inageku, Chiba 263-8522, Japan, National Institute for Materials Science (NIMS), 1-2-1 Sengen, Tsukuba 305-0047, Japan, and PRESTO, Japan Science and Technology Agency (JST), 4-1-8 Honcho Kawasaki, Saitama, Japan

Received March 28, 2010; E-mail: nakanishi.takashi@nims.go.jp

Near-infrared (NIR) light has been used in telecommunication, sensing, ablation, and biology.[1] Along these lines, single-walled carbon nanotubes (SWCNT) can also absorb NIR light, rapidly transferring electronic excitations into molecular vibration energies which induce heat.[2] This photothermal phenomenon has great potential for a wide range of applications, such as drug delivery systems and cancer therapies,[3] remote thermal reactions,[4] phase transitions of polymer gel hybrids,[5] and so forth.[6] But for each application, a proper temperature range is required. It is generally accepted that the laser-induced heating of SWCNT can generate temperature changes on the order of several tens of degrees centigrade, but it is not clear whether SWCNT can photothermally produce even higher temperatures. In aqueous solution, the temperature rise can be measured by a fluorescence technique.[7] However, measurements of the temperature increase in air, especially for areas of micrometer scale, can be challenging. One promising strategy for assessing temperature functions is through the use of a homologous series of materials with defined melting points. Thus, if the temperature reaches these melting points, the morphology changes of the micrometer-sized materials should be "visible" via various microscopy techniques during the photothermal conversion.

Here we show that microparticles, or microdisks, containing SWCNT and alkylated-fullerene (C_{60}) derivatives can be developed as a temperature indicator. Moreover, we reveal that NIR-induced SWCNT heating in air can reach temperatures as high as 220 °C when using SWCNT as a light antenna within a matrix of C_{60} derivatives. Additionally, C_{60} derivatives[8] with aliphatic chains of varying chain length or number (**1**−**3** in Figure 1a) possess different melting temperatures. In this way, heating elements are inserted at defined concentrations, and local melting can be evaluated by scanning probe, electron microscopy, or optical microscopy. Due to their dimensions, highly photostable carbon nanotubes can be inserted into assembled lamellae (Figure 1b) of the hydrophobic fullerene matrix. Although nanocarbon assembly[9] has been reported for various applications, such as energy conversion,[10] to the best of our knowledge this is the first report utilizing a fullerene-SWCNT assembly as the indicator for photothermal conversion of SWCNT.

SWCNT have reasonably high absorbance in the NIR region. The extinction coefficient, ε, of SWCNT solubilized by derivative **1** in THF at $\lambda = 830$ nm is about 15.4 L/g·cm; however, no absorption occurs with only **1** at the same wavelength [Figure S1, Supporting Information (SI)]. Thus, photothermal conversion by

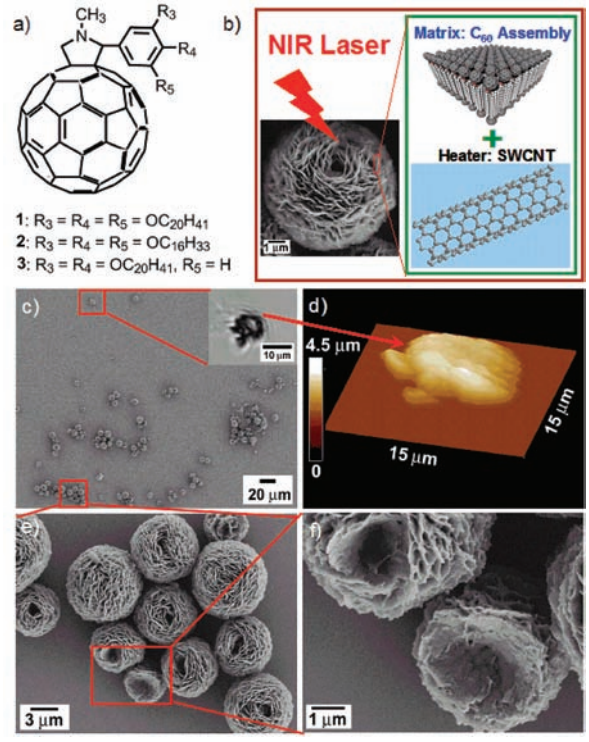

Figure 1. (a) Chemical structure of alkylated-C_{60} derivatives (**1**−**3**); (b) scheme of the fullerene-SWCNT assembly for evaluating photothermal conversion of SWCNT; (c) SEM image of **1**-SWCNT assembly [inset shows the optical image of an assembly illuminated by a NIR laser (90 mW)]; (d) AFM image of the same **1**-SWCNT assembly as in the inset to panel c; (e) SEM image of zoomed-in area of panel c selectively illuminated by a NIR laser (50 mW); and (f) enlarged area of panel e.

SWCNT could be exploited at a single wavelength by using an 830 nm laser (see details in SI).

Figure 1c,e shows scanning electron microscopy (SEM) images of the C_{60} derivative (**1**)-SWCNT flake-shaped microparticles. Preparation of maximum SWCNT content in the particles was optimized by heating 1,4-dioxane solution containing **1** (1.7 mg, 1 mM) and SWCNT (0.1 mg, ~6 wt %, HiPco) to 70 °C for 30 min with ultrasonication followed by cooling to room temperature. The flake-shaped microstructures (1−5 μm) of **1**-SWCNT are identical to those of **1** without SWCNT,[8a] which indicates the possibility for monitoring the microheating of a SWCNT-containing system using proper microscopy techniques. Upon NIR laser illumination at 50 mW, the flake-shaped surfaces of **1**-SWCNT assemblies started to "deform", while unexposed particles maintained their morphology (Figure 1e,f). Increasing the laser intensity (90 mW)

[†] Max Planck Institute of Colloids and Interfaces.
[‡] Chiba University.
[§] NIMS.
[⊥] JST.

10.1021/ja1026024

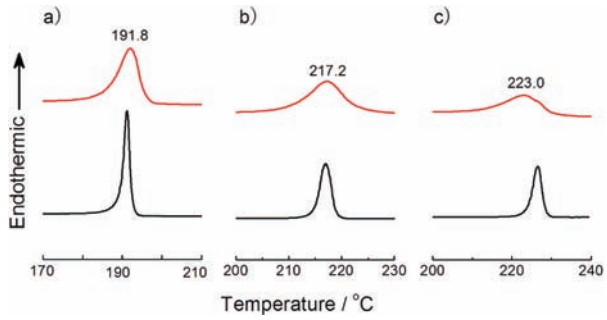

Figure 2. (a) DSC thermograms for the first heating of (a) **1**, (b) **2**, and (c) **3** with (red line) and without (black) SWCNT at a scanning rate of 10 °C/min.

destroyed the microparticles immediately, as visualized by optical (Figure 1c inset) and atomic force microscopy (AFM) (Figure 1d) observations. In the control experiment consisting of only **1**, microparticles with similar morphology did not transform the flake-shaped surface upon NIR laser irradiation, thus confirming the key role of SWCNT in the photothermal conversion.

In order to explore the relationship between the morphology change and the temperature rise upon NIR laser illumination, the **1**-SWCNT assembly was further analyzed by differential scanning calorimetry (DSC), FT-IR, X-ray diffraction (XRD), high-resolution cryogenic transmission electron microscopy (HR-cryo-TEM), and AFM. A DSC thermogram on the first heating trace of **1**-SWCNT shows two endothermic peaks. These two peaks correspond to the mesomorphic-to-isotropic (191.8 °C, Figure 2a) and crystalline-to-mesomorphic phase transitions (71.1 °C, Figure S2, SI), respectively, both of which are similar to those of **1** itself.[8b] The peaks became slightly broader due to the effect of SWCNT doping on the organized lamellar structure of **1**. At room temperature, the FT-IR spectrum displays CH_2 stretching vibrations at 2918 and 2850 cm^{-1}, indicating the crystalline state of the alkyl chain moieties in the microparticle assembly (Figure S3, SI). Furthermore, temperature-dependent XRD patterns (from room temperature to the isotropic phase transition temperature) show fine lamellar organization of **1** in the assembly. Flake-shaped microparticles of **1**-SWCNT exhibit moderately ordered lamellar structure in the solid state with a *d*-spacing of 4.5 nm (black lines in Figure 3a). HR-cryo-TEM observation further confirms the lamellar organization of the solid state (Figure 3b). When the temperature is increased (e.g., up to 170 °C), a highly ordered lamellar mesophase appears with a layer distance of 5.2 nm (blue lines). However, once the temperature is above that at which the isotropic phase transition occurs (e.g., at 210 °C), all intensive XRD peaks disappear (red line in Figure 3a). These results indicate the correspondence between the isotropic phase transition and the melting point of the assembly. Therefore, upon NIR laser irradiation, deformation of the **1**-SWCNT assembly is attributed to the temperature rise up to the melting point of **1**-SWCNT (i.e., 190 °C).

In addition, it is worth noting that effective sensing of the temperature rise upon NIR laser irradiation should also be attributed to the attractive interaction between alkylated-C_{60} derivatives and SWCNT. The assembly of C_{60} derivatives with SWCNT facilitates the unbundling and dispersion of SWCNT in organic solvents such as THF (Figure S4, SI). TEM observation reveals that the C_{60} derivatives can position themselves at the SWCNT surface (Figure S5, SI). This result is corroborated by AFM observation. As shown in Figure 3c, spin-coating **1**-SWCNT THF solution onto a Si substrate results in adsorption of **1** along the surface of SWCNT. It has been reported that many molecules bearing long alkyl chains

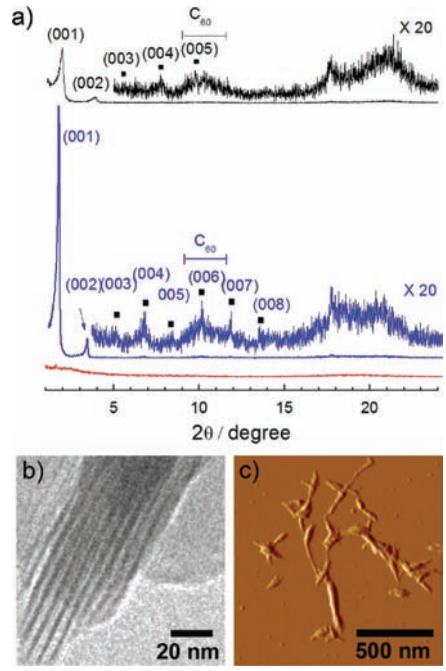

Figure 3. (a) X-ray diffraction patterns of **1**-SWCNT flake-shaped microparticles at room temperature in the solid state (black), in the lamellar mesophase at 170 °C (blue), and in the isotropic phase at 210 °C (red); (b) HR-cryo-TEM image of a **1**-SWCNT flake-shaped microparticle edge piece; and (c) AFM image of **1**-SWCNT spin-coated from diluted THF solution onto a Si surface.

form perfectly ordered and self-organized lamellar nanostructures on highly oriented pyrolytic graphite.[11] This is due to the close lattice matching between alkyl chains and graphite, which results in epitaxial growth of the long alkyl chain.[11] Previously, we found that alkylated-C_{60} derivatives self-organize onto a graphite surface to form straight nanowires.[12] The assembly of alkylated-C_{60} onto the graphite surface indicates that there are several attractive intermolecular forces, such as $\pi-\pi$ interactions between neighboring C_{60} moieties and at the C_{60}-graphite surface, as well as dispersion forces resulting from the long alkyl tails' high affinity for the graphite lattice. Due to the similar surface structures of graphite and SWCNT, we speculate that there are analogous interactions between **1** and SWCNT. These interactions enable SWCNT to disperse uniformly in the matrix of **1** within the microparticles, such that the total assembly can be used as a sensitive indicator.

In order to determine if NIR-induced SWCNT heating could reach higher temperatures, fullerene-SWCNT microparticles and microdisks comprising alkylated-C_{60} derivatives (**2** and **3**), possessing higher melting points, were prepared by similar procedures. DSC analysis (Figure 2b,c) revealed the melting points of **2**-SWCNT and **3**-SWCNT to be 217.2 and 223.0 °C, respectively. A **2**-SWCNT microdisk (Figure 4a, 2−8 μm) and a **3**-SWCNT flake-shaped microparticle (Figure 4d, 2−4 μm) were deformed upon lower power NIR laser illumination (50 mW), as shown in Figure 4b,e. Upon increasing the laser power (90 mW), the **2**-SWCNT microdisk and the **3**-SWCNT microparticle each opened a "hole" in the middle, exposing SWCNT. These results demonstrate that the morphology of the fullerenes may change, but that of the SWCNT does not (Figure 4c,f; see enlarged images in Figure S6, SI). NIR irradiation of a fullerene-SWCNT assembly in air can reach a local temperature in excess of around 220 °C.

It should be noted here that deformation of the micrometer-scale fullerene-SWCNT assembly can easily be visualized by optical

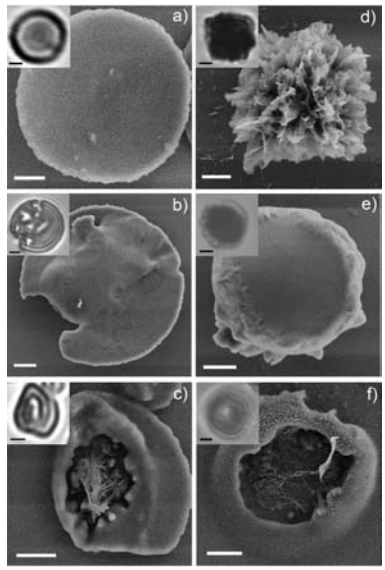

Figure 4. SEM images of (a−c) **2**-SWCNT and (d−f) **3**-SWCNT, (a,d) before NIR laser irradiation and after (b,e) lower power (50 mW) and (c,f) higher power (90 mW) NIR laser irradiation. Insets show the corresponding optical microscopy images. Scale bars are 1 μm.

microscopy (insets in Figure 4), thus providing great convenience in monitoring temperature *in situ* during photothermal conversion. Moreover, the assembly melting point can be tuned to a desired range by selecting an appropriate C_{60} derivative alkyl chain length or number of alkyl chains. Besides these findings using SWCNT, the methodology described here is also applicable to fullerene-multiwalled carbon nanotubes (MWCNT) assemblies (e.g., **1**-MWCNT, Figure S7, SI). Thus, fullerene-CNT assembly provides an unambiguous way to confirm the temperature rise in air upon NIR light irradiation. While this introduced technique facilitates the sensing of increasing temperature, irreversible morphology changes also occur in the samples.

In conclusion, a "temperature indicator" for photothermal conversion of carbon nanotubes in air upon NIR light irradiation is proposed by constructing an assembly of micrometer-sized, alkylated C_{60}-carbon nanotubes. This is based upon the notion that temperature rise can be confirmed via the melt-induced morphological change of "nanocarbons" assembly. Although various C_{60}-based micro- and nanoaggregates with potential future applications have been reported,[13] this work is one of the first examples in which the structural and organizational properties of such materials have been clearly shown to be potentially usable for a real application. We anticipate that the results presented here will lead to a wide range of applications, especially those associated with temperature rise via NIR light illumination. Moreover, considering that carbon nanotubes are widely used in biology for local heating, with operations conducted in an aqueous solution around body temperature,[3] our studies serve as a reminder that NIR light irradiation of carbon nanotubes can induce an extreme temperature rise in air as high as 220 °C. Further efforts will be made to investigate this mechanism in the current system by theoretical calculation. Also, a detailed study about the local heating behavior of fullerene-CNT assembly under various conditions, such as in different media, is underway.

Acknowledgment. This work was supported, in part, by a Grant-in-Aid for Scientific Researches from the Ministry of Education, Sciences, Sports and Culture, Japan, and PRESTO, JST, Japan (T.N.). Y.S. gratefully acknowledges JSPS for the Postdoctoral Fellowships for Foreign Researchers. We thank Dr. K. Yoshida (Kyoto-Advanced Nanotechnology network) for technical support with the TEM measurements and Dr. M. Takeuchi (NIMS) for useful discussion.

Supporting Information Available: Experimental details, UV−vis spectra of **1** and **1**-SWCNT in THF, DSC and FTIR of **1**-SWCNT microparticles, TEM of **1**-SWCNT, photo of **3**-SWCNT in THF, SEM and DSC for **1**-MWCNT microparticles, and complete ref 9c. This material is available free of charge via the Internet at http://pubs.acs.org.

References

(1) Skirtach, A. G.; Javier, A. M.; Kreft, O.; Köhler, K.; Alberola, A. P.; Möhwald, H.; Parak, W. J.; Sukhorukov, G. B. *Angew. Chem., Int. Ed.* **2006**, *45*, 4612.

(2) (a) Miyako, E.; Nagata, H.; Hirano, K.; Hirotsu, T. *Angew. Chem., Int. Ed.* **2008**, *47*, 3610. (b) Singh, P.; Campidelli, S.; Giordani, S.; Bonifazi, D.; Bianco, A.; Prato, M. *Chem. Soc. Rev.* **2009**, *38*, 2214.

(3) (a) Kam, N. W. S.; O'Connell, M.; Wisdom, J. A.; Dai, H. *Proc. Natl. Acad. Sci. U.S.A.* **2005**, *102*, 11600. (b) Ghosh, S.; Dutta, S.; Gomes, E.; Carroll, D.; Agostino, R.; Olson, J.; Guthold, M.; Gmeiner, W. H. *ACS Nano* **2009**, *3*, 2667.

(4) (a) Miyako, E.; Itoh, T.; Nara, Y.; Hirotsu, T. *Chem.—Eur. J.* **2009**, *15*, 7520. (b) Pastine, S. J.; Okawa, D.; Zettl, A.; Fréchet, J. M. J. *J. Am. Chem. Soc.* **2009**, *131*, 13586.

(5) Fujigaya, T.; Morimoto, T.; Niidome, Y.; Nakashima, N. *Adv. Mater.* **2008**, *20*, 3610.

(6) Barone, P. W.; Baik, S.; Heller, D. A.; Strano, M. S. *Nat. Mater.* **2005**, *4*, 86.

(7) Skirtach, A. G.; Dejugnat, C.; Braun, D.; Susha, A. S.; Rogach, A. L.; Parak, W. J.; Möhwald, H.; Sukhorukov, G. B. *Nano Lett.* **2005**, *5*, 1371.

(8) (a) Nakanishi, T.; Michinobu, T.; Yoshida, K.; Shirahata, N.; Ariga, K.; Möhwald, H.; Kurth, D. G. *Adv. Mater.* **2008**, *20*, 443. (b) Nakanishi, T.; Shen, Y.; Wang, J.; Yagai, S.; Funahashi, M.; Kato, T.; Fernandes, P.; Möhwald, H.; Kurth, D. G. *J. Am. Chem. Soc.* **2008**, *130*, 9236. (c) Nakanishi, T. *Chem. Commun.* **2010**, *46*, 3425.

(9) (a) Xu, Y. F.; Liu, Z. B.; Zhang, X. L.; Wang, Y.; Tian, J. G.; Huang, Y.; Ma, Y. F.; Zhang, X. Y.; Chen, Y. S. *Adv. Mater.* **2009**, *21*, 1275. (b) Ballesteros, B.; Torre, G.; Ehli, C.; Aminur Rahman, G. M.; Agulló-Rueda, F.; Guldi, D. M.; Torres, T. *J. Am. Chem. Soc.* **2007**, *129*, 5061. (c) Nasibulin, A. G.; et al. *Nat. Nanotechnol.* **2007**, *2*, 156. (d) Giordani, S.; Colomer, J. F.; Cattaruzza, F.; Alfonsi, J.; Meneghetti, M.; Prato, M.; Bonifazi, D. *Carbon* **2009**, *47*, 578. (e) Koshino, M.; Solin, N.; Tanaka, T.; Isobe, H.; Nakamura, E. *Nat. Nanotechnol.* **2008**, *3*, 595. (f) Krishna, V.; Stevens, N.; Koopman, B.; Moudgil, B. *Nat. Nanotechnol.* **2010**, *5*, 330. (g) Takaguchi, Y.; Tamura, M.; Sako, Y.; Yanagimoto, Y.; Tsuboi, S.; Uchida, T.; Shimamura, K.; Kimura, S.; Wakahara, T.; Maeda, Y.; Akasaka, T. *Chem. Lett.* **2005**, *34*, 1608.

(10) (a) D'Souza, F.; Chitta, R.; Sandanayaka, A. S. D.; Subbaiyan, N. K.; D'Souza, L.; Araki, Y.; Ito, O. *J. Am. Chem. Soc.* **2007**, *129*, 15865. (b) Umeyama, T.; Tezuka, N.; Fujita, M.; Hayashi, S.; Kadota, N.; Matano, Y.; Imahori, H. *Chem.—Eur. J.* **2008**, *14*, 4875. (c) Guldi, D. M.; Menna, E.; Maggini, M.; Marcaccio, M.; Paolucci, D.; Paolucci, F.; Campidelli, S.; Prato, M.; Aminur Rahman, G. M.; Schergna, S. *Chem.—Eur. J.* **2006**, *12*, 3975.

(11) (a) Rabe, J. P.; Buchholz, S. *Science* **1991**, *253*, 424. (b) Miyashita, N.; Möhwald, H.; Kurth, D. G. *Chem. Mater.* **2007**, *19*, 4259.

(12) (a) Nakanishi, T.; Miyashita, N.; Michinobu, T.; Wakayama, Y.; Tsuruoka, T.; Ariga, K.; Kurth, D. *J. Am. Chem. Soc.* **2006**, *128*, 6328. (b) Nakanishi, T.; Takahashi, H.; Michinobu, T.; Takeuchi, M.; Teranishi, T.; Ariga, K. *Colloids Surf., A* **2008**, *321*, 99.

(13) (a) Zhang, X.; Takeuchi, M. *Angew. Chem., Int. Ed.* **2009**, *48*, 9646. (b) Laiho, A.; Ras, R. H. A.; Valkama, S.; Ruokolainen, J.; Osterbacka, R.; Ikkala, O. *Macromolecules* **2006**, *39*, 7648. (c) Matsuo, Y.; Sato, Y.; Niinomi, T.; Soga, I.; Tanaka, H.; Nakamura, E. *J. Am. Chem. Soc.* **2009**, *131*, 16048. (d) Yamamoto, Y.; Zhang, G.; Jin, W.; Fukushima, T.; Ishii, N.; Saeki, A.; Seki, S.; Tagawa, S.; Minari, T.; Tsukagoshi, K.; Aida, T. *Proc. Natl. Acad. Sci. U.S.A.* **2009**, *106*, 21051.

JA1026024